Electronic Supplementary Information for:

Single-component molecular conductor [Pt(dmdt)$_2$] — A three-dimensional ambient-pressure molecular Dirac electron system

Biao Zhou,[a] Shoji Ishibashi,[b] Tatsuru Ishii,[a] Takahiko Sekine,[c] Ryosuke Takehara,[c] Kazuya Miyagawa,[c] Kazushi Kanoda,[c] Eiji Nishibori[d] and Akiko Kobayashi*[a]*

a. *Department of Chemistry, College of Humanities and Sciences, Nihon University, Setagaya-Ku, Tokyo 156-8550, Japan. e-mail: zhou@chs.nihon-u.ac.jp, akoba@chs.nihon-u.ac.jp*

b. *Research Center for Computational Design of Advanced Functional Materials (CD-FMat), National Institute of Advanced Industrial Science and Technology (AIST), Tsukuba 305-8568, Japan.*

c. *Department of Applied Physics, University of Tokyo, Bunkyo-ku, Tokyo 113-8656, Japan*

d. *Faculty of Pure and Applied Science and Tsukuba Research Center for Energy Materials Science (TREMS), University of Tsukuba, Tsukuba 305-8571, Japan.*

Experimental details

Sample Preparations

All of the synthetic experiments were performed with Schlenk techniques under an argon atmosphere. The starting material $(Me_4N)_2[Pt(dmdt)_2]$, was prepared following the previously reported procedure,[1,2] with the platinum source trans-bis(benzonitrile)dichloroplatinum(II) $[PtCl_2(PhCN)_2]$. The neutral $[Pt(dmdt)_2]$ crystals were obtained by electrochemical oxidation from an acetonitrile solution with a constant current of 0.4 μA at room temperature in standard glass H-type cells. Air-stable black thin-plate single crystals with sizes less than 70 μm grown on the anode within approximately 4 weeks (Fig. S7a).

X-ray Structural Determinations

The crystal structures of neutral $[Pt(dmdt)_2]$ were determined by the single crystal X-ray diffraction studies using a Rigaku Micro7HFM-VariMax Saturn 724R CCD system equipped with a confocal X-ray mirror at room temperature. The crystal data for $[Pt(dmdt)_2]$ are as follows: CCDC 1889632, $C_{16}H_{12}S_{12}Pt_1$, M = 784.08, triclinic, space group *P*–1 (No. 2), a = 6.620(1) Å, b = 7.611(2) Å, c = 11.639(4) Å, α = 86.05(3)°, β = 78.98(3)°, γ = 75.04(3)°, V = 556.0(3) Å^3, and Z = 1. Details of the structure determination are listed in Table S1. Selected bond lengths and angles are listed in Table S2. Atomic coordinates are listed in Table S3. The crystal data and the purity of the samples were confirmed by synchrotron radiation powder X-ray diffraction experiments at the BL02B2 in the SPring-8 facility (Fig. S7b).

Electrical Resistivity Measurements

Four-probe resistivity measurements were performed on compressed pellets of polycrystalline samples of $[Pt(dmdt)_2]$ in the temperature range of 4.2−298 K. Annealed gold wires (10 μm in diameter) bonded to the sample by gold paint were used as leads. Two-probe resistivity measurements were also conducted using very small and thin single crystals with a size of approximately 65 μm.

Magnetic Susceptibility Measurements

Magnetic susceptibility measurements of $[Pt(dmdt)_2]$ were collected with a Quantum Design MPMS-7XL super-conducting quantum interference device (SQUID) magnetometer in the temperature range of 2.0−300 K. The applied magnetic field was 5000 Oe. The samples were wrapped in clean aluminum foil whose magnetic susceptibility was separately measured and subtracted. The diamagnetic contribution was estimated from Pascal's constants[3] to be -3.2×10^{-4} emu·mol^{-1}.

First-principles DFT calculations

First-principles DFT calculations using the QMAS (Quantum MAterials Simulator) code[4] based on the projector augmented-wave (PAW) method[5] and plane-wave basis set. As for the exchange-

correlation functional, we used the generalized gradient approximation (GGA) by Perdew, Burke and Ernzerhof.[6] The atomic positions were computationally optimized with the *P*1 space group, so that the maximum force amplitude was less than 5×10^{-5} Ha/bohr. Optimized fractional atomic coordinates are listed in Table S4, which are very consistent with that of single crystal X-ray diffraction determination. The plane-wave cutoff energy was set to 20 Ha. For self-consistent calculations, $12 \times 12 \times 6$ *k* points in the full Brillouin zone were sampled.

1. B. Zhou, A. Kobayashi, Y. Okano, T. Nakashima, S. Aoyagi, E. Nishibori, M. Sakata, M. Tokumoto and H. Kobayashi, *Adv. Mater.*, 2009, **21**, 3596-3600.
2. A. Kobayashi, H. Tanaka and H. Kobayashi, *J. Mater. Chem.*, 2001, **11**, 2078-2088.
3. Y. Iwasawa, *Handbook of Chemistry: Pure Chemistry 5th ed.*, Maruzen, Tokyo, 2004.
4. S. Ishibashi, T. Tamura, S. Tanaka, M. Kohyama and K. Terakura, *Phys. Rev. B*, 2007, **76**, 153310.
5. P. E. Blöchl, *Phys. Rev. B*, 1994, **50**, 17953-17979.
6. J. P. Perdew, K. Burke and M. Ernzerhof, *Phys. Rev. Lett.*, 1996, **77**, 3865-3868.

Table S1 X-ray Crystallographic Data of [Pt(dmdt)$_2$] (CCDC 1889632)

T (K)		298
Empirical Formula		$C_{16}H_{12}PtS_{12}$
Formula Weight		784.08
Crystal System		triclinic
Space Group		P-1 (#2)
Lattice Parameters	a (Å)	6.6200(12)
	b	7.611(2)
	c	11.639(4)
	α (°)	86.05(3)
	β	78.98(3)
	γ	75.04(3)
	V (Å^3)	556.0(3)
Z value		1
D_{calc} (g/cm^3)		2.341
μ(Mo Kα) (mm^{-1})		7.416
Diffractometer		Rigaku Saturn724
Radiation		Mo Kα (λ = 0.71075 Å)
No. of Reflections Measured		
Total		6426
Unique		2499
No. Observations (I>2σ)		1662
No. Variables		93
Residuals: R_1 (I>2σ)[a]		0.116
Residuals: wR_2 (I>2σ)[b]		0.301
GOF Indicator		1.011

[a] $R_1 = \sum||F_o| - |F_c||/\sum|F_o|$ [b] $wR_2 = [\sum\omega(|F_o| - |F_c|)^2/\sum\omega F_o^2]^{1/2}$

Table S2 Selected bond lengths and angles of [Pt(dmdt)$_2$]

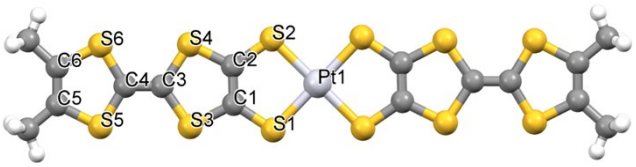

Pt1-S1	2.308(6) Å
Pt1-S2	2.293(5)
C1-C2	1.37(2)
C3-C4	1.34(3)
C5-C6	1.35(3)
S1-Pt1-S2	90.28(17)°

Table S3 Fractional Atomic Coordinates of [Pt(dmdt)$_2$] by single crystal X-ray diffraction determination

Number	Atom	X-frac.	Y-frac.	Z-frac.
1	Pt1	0	0	0
2	S1	0.2612(7)	0.0073(7)	0.1043(4)
3	S2	-0.2571(7)	0.1108(7)	0.1578(4)
4	S3	0.2365(7)	0.1248(8)	0.3487(5)
5	S4	-0.2311(7)	0.2206(7)	0.3954(5)
6	S5	0.2300(7)	0.2728(7)	0.6050(4)
7	S6	-0.2333(7)	0.3726(8)	0.6475(5)
8	C1	0.111(2)	0.094(3)	0.2330(15)
9	C2	-0.106(3)	0.137(3)	0.2576(17)
10	C3	0.004(3)	0.221(3)	0.4499(13)
11	C4	0.001(3)	0.278(3)	0.5564(13)
12	C5	0.102(3)	0.359(3)	0.742(2)
13	C6	-0.112(3)	0.412(3)	0.7603(18)
14	C7	0.241(5)	0.377(4)	0.814(3)
15	C8	-0.265(5)	0.487(4)	0.859(3)
16	H1	0.21	0.3155	0.8873
17	H2	0.224	0.5035	0.8268
18	H3	0.3842	0.3241	0.7764
19	H4	-0.2419	0.6004	0.8774
20	H5	-0.2521	0.4044	0.9245
21	H6	-0.4055	0.508	0.8409

Table S4 Fractional Atomic Coordinates of [Pt(dmdt)$_2$] by computationally optimized*

Number	Atom	X-frac.	Y-frac.	Z-frac.
1	Pt1	0	0	0
2	S1	0.259744	0.013165	0.103845
3	S2	-0.25711	0.114048	0.158357
4	S3	0.235671	0.126114	0.349705
5	S4	-0.23118	0.224189	0.396252
6	S5	0.230944	0.27413	0.60654
7	S6	-0.23278	0.374672	0.649394
8	C1	0.112195	0.09727	0.235371
9	C2	-0.10762	0.141564	0.258108
10	C3	0.001923	0.218705	0.445824
11	C4	0.000723	0.28216	0.553837
12	C5	0.104253	0.360969	0.743781
13	C6	-0.11115	0.407795	0.763852
14	C7	0.243561	0.373437	0.828104
15	C8	-0.25415	0.482215	0.873767
16	H1	0.172366	0.336713	0.916535
17	H2	0.267775	0.511119	0.828837
18	H3	0.399507	0.276576	0.807248
19	H4	-0.16102	0.507815	0.935963
20	H5	-0.34479	0.384971	0.915061
21	H6	-0.36778	0.610995	0.857444
22	S7	-0.25974	-0.01317	-0.10385
23	S8	0.257114	-0.11405	-0.15836
24	S9	-0.23567	-0.12611	-0.34971
25	S10	0.231183	-0.22419	-0.39625
26	S11	-0.23094	-0.27413	-0.60654
27	S12	0.232784	-0.37467	-0.64939

28	C9	-0.1122	-0.09727	-0.23537
29	C10	0.107619	-0.14156	-0.25811
30	C11	-0.00192	-0.21871	-0.44582
31	C12	-0.00072	-0.28216	-0.55384
32	C13	-0.10425	-0.36097	-0.74378
33	C14	0.111151	-0.4078	-0.76385
34	C15	-0.24356	-0.37344	-0.8281
35	C16	0.254152	-0.48222	-0.87377
36	H7	-0.17237	-0.33671	-0.91654
37	H8	-0.26778	-0.51112	-0.82884
38	H9	-0.39951	-0.27658	-0.80725
39	H10	0.161024	-0.50782	-0.93596
40	H11	0.344787	-0.38497	-0.91506
41	H12	0.367779	-0.611	-0.85744

*The atomic positions were computationally optimized with the *P*1 space group.

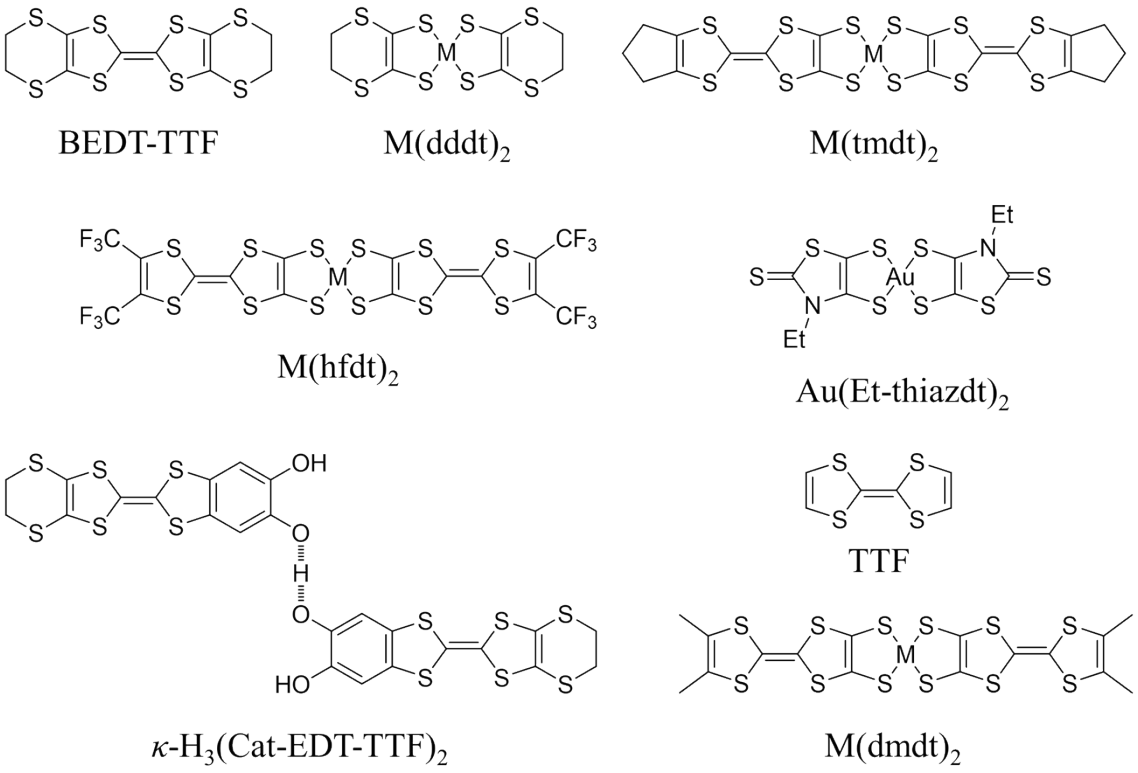

Fig. S1 Molecules and the abbreviations. BEDT-TTF = Bis(ethylenedithio)tetrathiafulvalene; dddt = 5,6-dihydro-1,4-dithiin-2,3-dithiolate; tmdt = trimethylenetetrathiafulvalenedithiolate; hfdt = bis(trifluoromethyl)tetrathiafulvalenedithiolate; Et-thiazdt = N-ethyl-1,3-thiazoline-2-thione-4,5-dithiolate; Cat-EDT-TTF = catechol-fused ethylenedithiotetrathiafulvalene; TTF = tetrathiafulvalene; dmdt = dimethyltetrathiafulvalenedithiolate.

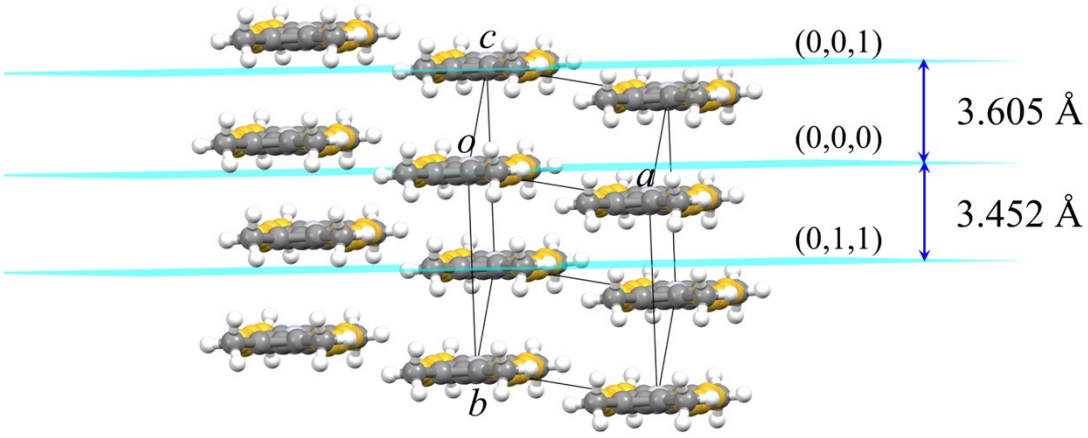

Fig. S2 The interplanar distance between the molecules on (0,0,0) and (0,0,1) is 3.605 Å, and molecules on (0,0,0) and (0,1,1) is 3.452 Å.

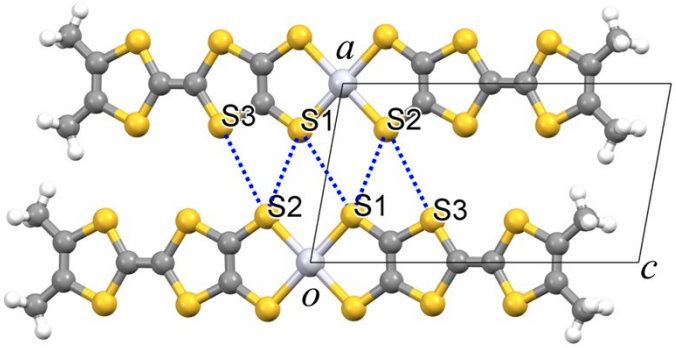

Fig. S3 There are many short S···S contacts shorter than the S···S van der Waals distance (3.70 Å) between the adjacent molecules along the *a*-axis. e.g. S1···S1 (3.581 Å), S1···S2 (3.647 Å), S2···S3 (3.631 Å).

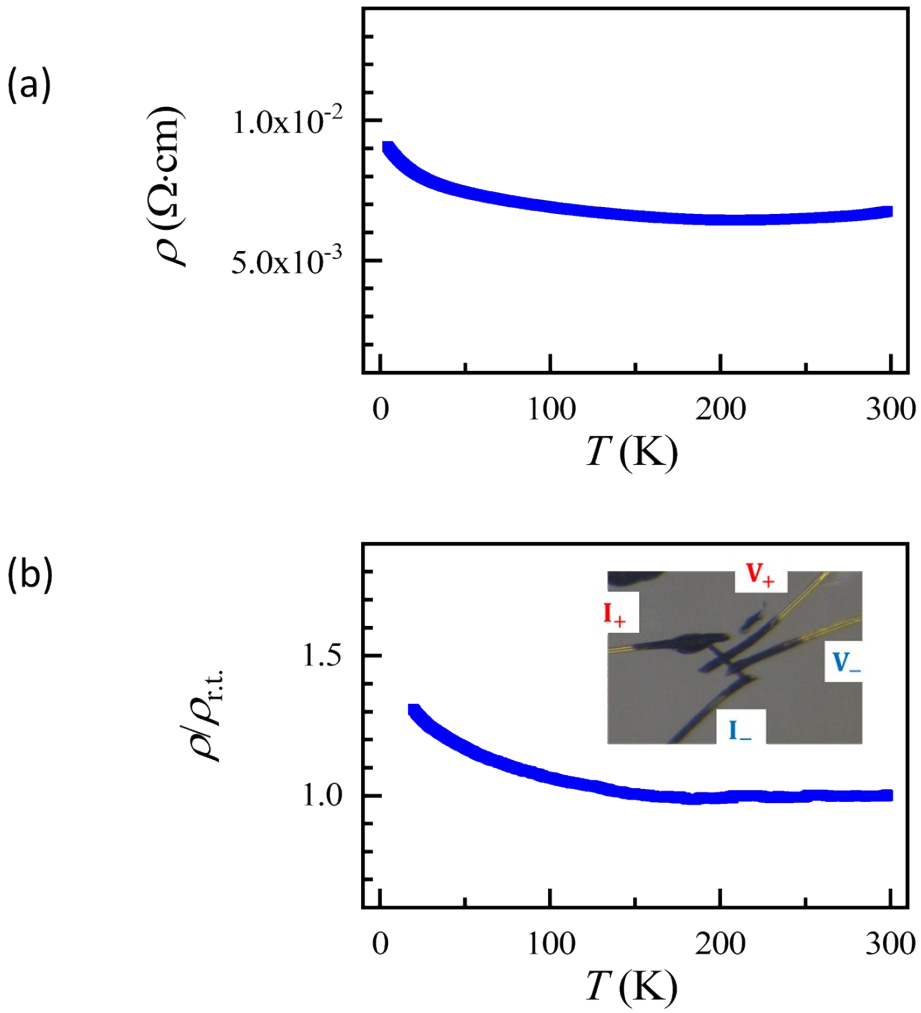

Fig. S4 (a) Temperature dependence of electrical resistivity of [Pt(dmdt)$_2$] performed on a compressed pellet using the conventional four-probe method at ambient pressure. (b) The single crystal resistivity measurement by two-probe methods with the crystal size 65 μm. The inset shows a photograph of a four-probe measurement of a [Pt(dmdt)$_2$] single crystal, however, due to cracks in the single crystal only two probes were working properly.

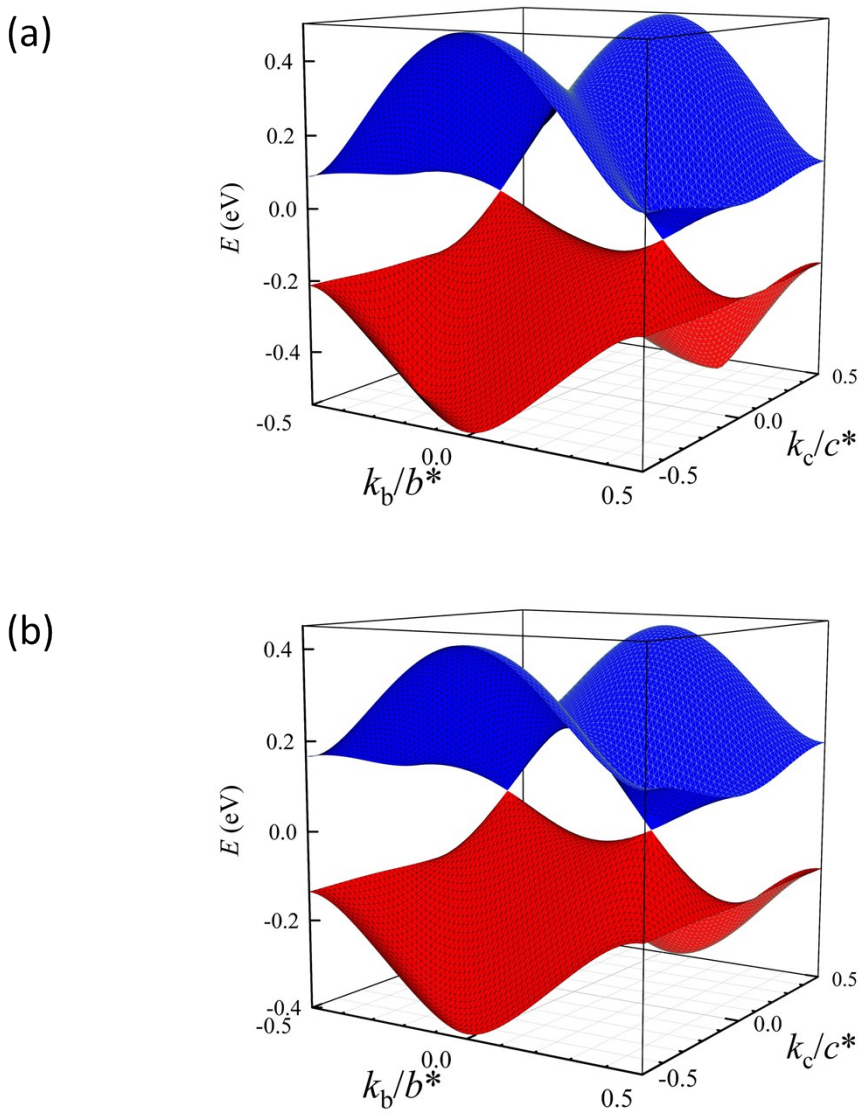

Fig. S5 The band energy dispersion surface of [Pt(dmdt)$_2$] in the first Brillouin zone. (a) Dirac cones emerge at the points of (k_b, k_c) = (0.381b*,–0.202c*) and (–0.381b*,0.202c*) for k_a = 0, (b) (k_b, k_c) = (–0.326b*,–0.160c*) and (–0.326b*,0.160c*) for k_a = ±½a*.

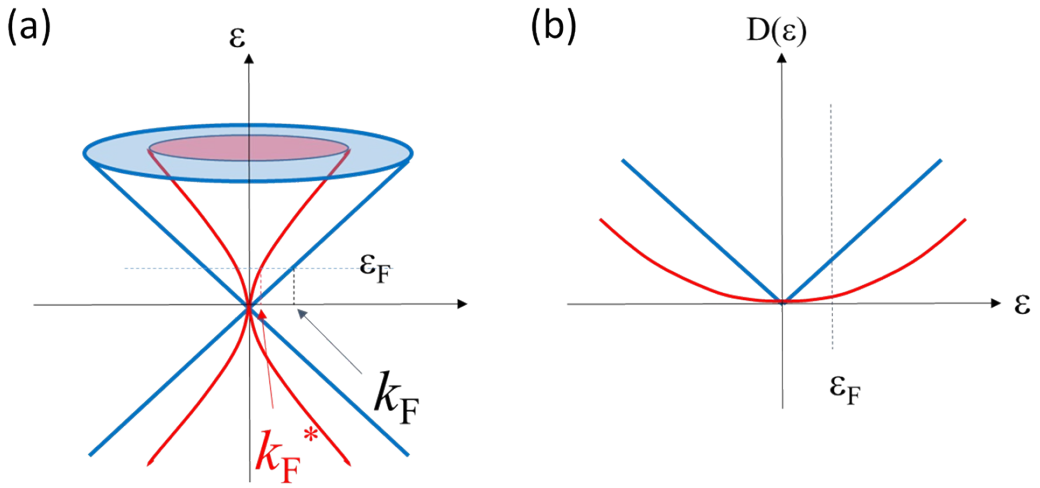

Fig. S6 (a) Reshaping of Dirac cone by long-range Coulomb repulsion. The blue cone is the dispersion relation expected for massless Dirac electrons without Coulomb interactions. In the presence of Coulomb interactions, the velocity of electron is renormalized logarithmically, leading to the cone reshaping as shown by red curves. The k_F of the uncorrelated Dirac cone corresponding to the Fermi energy, ε_F, is reduced to k_F*, approaching the Dirac point, by the cone reshaping due to long-range Coulomb interactions. (b) Density of states for massless Dirac electrons in the absence (blue lines) and presence (red curve) of Coulomb interaction among electrons. The density of states of uncorrelated massless Dirac electrons at the Fermi energy, ε_F, is reduced by the long-range Coulomb interactions.

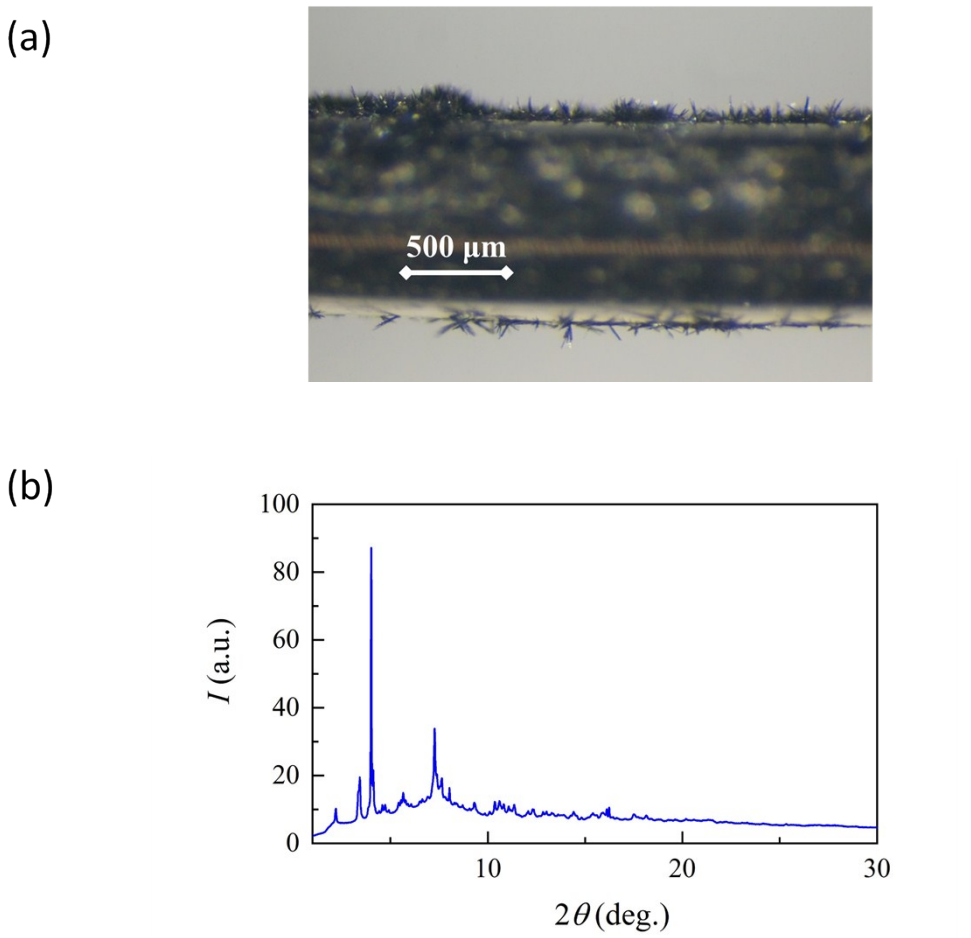

Fig. S7 (a) The photograph of the single crystals of [Pt(dmdt)$_2$] growing on the electrode. (b) The synchrotron radiation X-ray powder diffraction patterns of [Pt(dmdt)$_2$] at room temperature with a wavelength of 0.4405416(8) Å